Received: 26 September 2017 | Revised: 25 February 2018 | Accepted: 27 February 2018

DOI: 10.1002/humu.23416

RESEARCH ARTICLE

WILEY HGVS HUMAN GENOME VARIATION SOCIETY

ABCA3 missense mutations causing surfactant dysfunction disorders have distinct cellular phenotypes

Ulrike Schindlbeck[1]* | Thomas Wittmann[1]* | Stefanie Höppner[1] | Susanna Kinting[1] | Gerhard Liebisch[2] | Jan Hegermann[3] | Matthias Griese[1]

[1]Dr. von Hauner Children's Hospital, Ludwig-Maximilians University, German Centre for Lung Research (DZL), Munich, Germany

[2]Institute for Clinical Chemistry and Laboratory Medicine, University of Regensburg, Regensburg, Germany

[3]Institute of Functional and Applied Anatomy, Hannover Medical School, German Center for Lung Research (DZL), Hannover, Germany

Correspondence
Matthias Griese, Dr. von Hauner Children's Hospital, Ludwig-Maximilians University, German Centre for Lung Research (DZL), Lindwurmstraße 2a, 80337 Munich, Germany.
Email: Matthias.Griese@med.uni-muenchen.de

Funding information
FöFoLe (Ludwig-Maximilians University)

Contract grant sponsors: German Center for Lung Research (DZL); German Research Foundation (DFG) (Gr 970/8-1); Ludwig-Maximilians University (FöFoLe 21/2013).

*Ulrike Schindlbeck and Thomas Wittmann contributed equally to this work.

Communicated by Peter K. Rogan

Abstract

Mutations in the ATP-binding cassette subfamily A member 3 (*ABCA3*) gene are the most common monogenetic cause of surfactant dysfunction disorders in newborns and interstitial lung diseases in children and young adults. Although the effect of mutations resulting in truncated or incomplete proteins can be predicted, the consequences of missense variants cannot be as easily. Our aim was to investigate the intracellular handling and disturbance of the cellular surfactant system in a stable cell model with several different clinically relevant ABCA3 missense mutations. We found that the investigated missense mutations within the *ABCA3* gene affect surfactant homeostasis in different ways: first by disrupting intracellular ABCA3 protein localization (c.643C > A, p.Q215K; c.2279T > G, p.M760R), second by impairing the lipid transport of ABCA3 protein (c.875A > T, p.E292V; c.4164G > C, p.K1388N), and third by yet undetermined mechanisms predisposing for the development of interstitial lung diseases despite correct localization and normal lipid transport of the variant ABCA3 protein (c.622C > T, p.R208W; c.863G > A, p.R288K; c.2891G > A, p.G964D). In conclusion, we classified cellular consequences of missense ABCA3 sequence variations leading to pulmonary disease of variable severity. The corresponding molecular pathomechanisms of such ABCA3 variants may specifically be addressed by targeted treatments.

KEYWORDS

ATP-binding cassette transporters, human ABCA3 protein, interstitial lung diseases, respiratory distress syndrome of the newborn, surfactant dysfunction

1 | INTRODUCTION

Interstitial lung diseases (ILD) in children comprise a broad array of chronic respiratory disorders with considerable morbidity and mortality (Griese et al., 2015a). Several monogenetic causes, mainly associated with disturbances of the pulmonary surfactant system, have been identified (Hartl & Griese, 2005), including mutations in the genes coding for surfactant proteins (*SFTPC*, *SFTPB*) (Griese et al., 2016; Nogee, 2004), thyroid transcription factor-1 (*NKX2-1*) (Kleinlein et al., 2011; Thorwarth et al., 2014), and ATP-binding cassette subfamily A member 3 (*ABCA3*, MIM# 601615), while mutations in *ABCA3* appear to be most frequent (Brasch et al., 2006; Saugstad et al., 2007).

Surfactant, a mixture of specific lipids and proteins is necessary for normal pulmonary gas exchange (Griese, 1999) and is produced by type II pneumocytes with the help of ABCA3 (Figure 1). This lipid transporter, localized in the limiting membrane of lamellar bodies (LBs) (Yamano et al., 2001), contains two transmembrane domains composed of six helices each, domains exposed into the LB lumen and domains in the cytoplasm with two nucleotide-binding sites hydrolyzing ATP (Figure 2). ABCA3 is essential for the specific assembly of pulmonary surfactant and the biogenesis and formation of LBs (Besnard et al., 2010; Cheong et al., 2007), as demonstrated ex vivo in patients with ABCA3 mutations (Shulenin et al., 2004) and in vitro in the alveolar type II cell models A549 and HEK293 after the expression of wild-type (WT) ABCA3 (Flamein et al., 2012).

To date, more than 200 different ABCA3 mutations have been identified in patients with surfactant dysfunction disorders (Beers & Mulugeta, 2017). They are classified into "null" mutations, including nonsense and frameshift mutations predicted to result in truncated or nonfunctional proteins, as well as "other" mutations, including in-frame insertion/deletions, splice site and missense mutations, whose effects on protein function are more difficult to predict (Wambach et al., 2014).

Cheong et al. (2006) initially suggested that ABCA3 missense mutations might lead to an impaired trafficking or dysfunction of the ABCA3 protein. Matsumura, Ban, Ueda, & Inagaki (2006) further distinguished type 1 mutations with an abnormal intracellular localization and type 2 mutations with decreased ATP hydrolysis despite

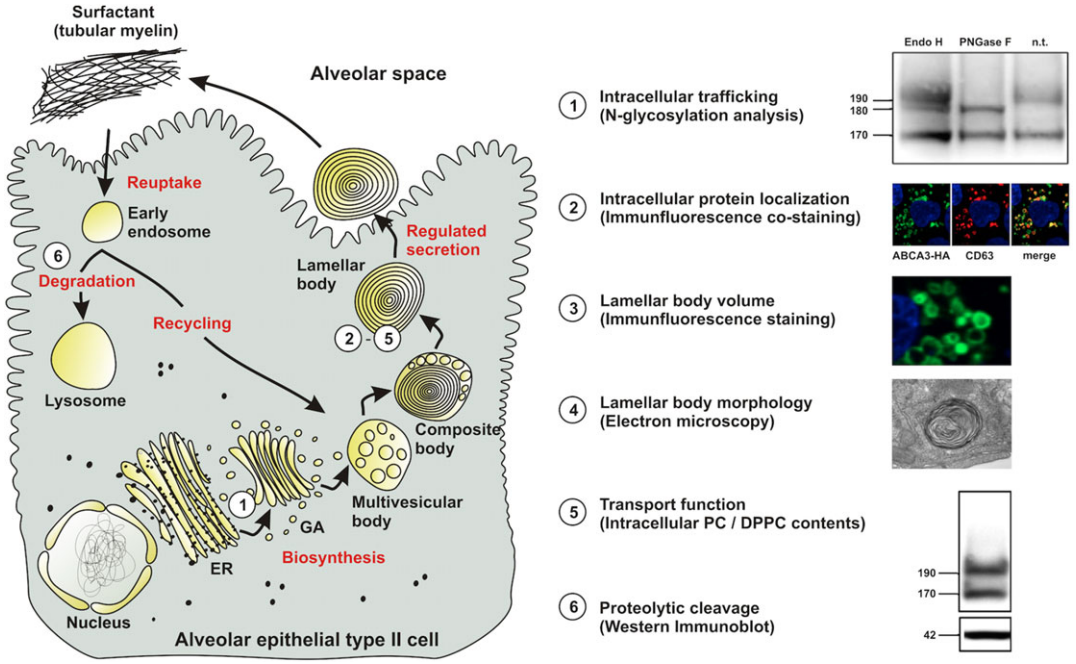

FIGURE 1 Overview of the ABCA3 protein pathway through the cell. Numbers indicate intracellular localization of tools used for classification and images on the right show examples of results obtained for ABCA3-HA WT. Illustration adapted from S. Kern. DPPC, dipalmitoylphosphatidylcholine; ER, endoplasmic reticulum; GA, Golgi apparatus; PC, phosphatidylcholine

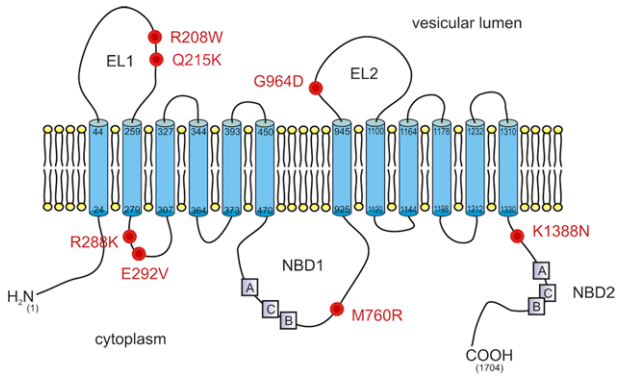

FIGURE 2 Schematic representation of the ABCA3 protein and localization of missense sequence variations investigated in this work. Illustration adapted from S. Kern. A, walker A motif; B, walker B motif; C, C motif; EL, extracellular loop; NBD, nucleotide binding domain

correct intracellular localization of ABCA3 protein. The compound heterozygous combination of type 1 and 2 mutations is currently discussed as type 3 mutations and often present with a more severe phenotype (Beers & Mulugeta, 2017).

Unfortunately, clinical data and in particular lung tissue or molecular investigations are not always available. In order to gain insight into the cellular phenotype, we developed a number of tools to assess cellular pathologies related to ABCA3 mutations in a previous study, where we could demonstrate close correlations between in vitro results and ex vivo data (Brasch et al., 2006; Campo et al., 2014; Wittmann et al., 2016a; Wittmann et al., 2016b).

In this study, we investigated in parallel several genetic missense variations of ABCA3, previously found in patients with surfactant dysfunction disorders of different disease severity. An overview of the cellular pathways addressed is illustrated in Figure 1. Our goal was to obtain a detailed understanding of the degree of cellular ABCA3 dysfunction in each case in the hope that this knowledge will be of great benefit for future subjects expressing similar variants.

2 | MATERIAL AND METHODS

2.1 | Generation of stable cell clones

Human A549 cells (German Collection of Microorganisms, DSMZ, Braunschweig, Germany) were cultured as previously described (Wittmann et al., 2016b). ABCA3-HA WT and the variations c.622C > T (p.R208W), c.643C > A (p.Q215K), c.863G > A (p.R288K), c.875A > T (p.E292V), c.2279T > G (p.M760R), c.2891G > A (p.G964D), and c.4164G > C (p.K1388N) were stably transfected into A549 cells using the *"Sleeping Beauty"* transposon system (Geurts et al., 2003). The variants are submitted to dbSNP (https://www.ncbi.nlm.nih.gov/projects/SNP/) and described using the NM_001089.2 transcript reference sequence. Nucleotide numbering uses +1 as the A of the ATG translation initiation codon in the reference sequence, with the initiation codon as codon 1. Cells were cotransfected with pCMV(CAT)T7-SB100 and the corresponding pT2/HB-puro-ABCA3-HA respectively, using Lipofectamine 3000 (Thermo Fisher Scientific, Waltham, Massachusetts, USA) according to the manufacturer's instructions. Detailed descriptions of the plasmid cloning method are given in the supplements. Selection of stable cells was started 48 hr after transfection by addition of 1 μg/ml Puromycin (Sigma Aldrich, Taufkirchen, Germany) and single cell clones were obtained by seeding isolated cells into each well of a 96-well plate.

2.2 | Immunoblotting

A549 cells were lysed in radioimmunoprecipitation assay buffer [0.15 M sodium chloride, 1% Triton X-100, 0.5% sodium deoxycholate, 0.1% sodium dodecylsulfate, 5 mM ethylenediaminetetraacetic acid (EDTA), 50 mM Tris (pH 8)] (all from Sigma except EDTA from GE Healthcare, Buckinghamshire, UK and Tris from Merck Millipore, Darmstadt, Germany) supplemented with complete protease inhibitor (PI; Roche, Mannheim, Germany). The lysates were then centrifuged and the protein concentration of the post-nuclear supernatant (PNS) was measured using the Pierce BCA protein assay. 20 μg of cell lysates were complemented with 4× LDS buffer (Invitrogen, Waltham, Massachusetts, USA) and 10% dithiothreitol (Sigma) and loaded on NuPage Mini 3%–8% Tris-Acetate gels (Invitrogen) for gel electrophoresis. Separated proteins were transferred to polyvinyledene fluoride membranes (Millipore). Membranes were blocked with 5% skim milk in TBS-T (Sigma) and incubated with primary antibody, followed by HRP-conjugated secondary antibody. All antibodies used are listed in the supplements. ECL reagent (GE Healthcare) was used for detection and relative density of separated protein bands was quantified using ImageJ software.

2.3 | N-glycosylation analysis

Harvested stably transfected cells were resuspended in 1 mM EDTA pH8.0 in PBS, supplemented with complete PI and homogenized in a Potter-Elvehjem homogenizer. Lysates were additionally sonicated for 40 sec and centrifuged (20 min, 700 × *g*, 4°C). The obtained PNS was further centrifuged (1 hr, 100.000 × *g*, 4°C) and the resulting total membrane fraction pellet was resuspended in 25 mM HEPES/NaOH pH7.0 in PBS, supplemented with PI. 20 μg of the total membrane fractions were denatured with 10× Glycoprotein Denaturing Buffer and treated with either EndoH or PNGaseF enzyme mix according to the manufacturer's instructions (NEB, Massachusetts, USA). The deglycosylated proteins were then separated and labeled with antibodies analogous to Immunoblotting. ABCA3-HA was detected using Femto reagent (Thermo Fisher Scientific), resulting protein bands were imaged with DIANAIII (Raytest, Straubenhardt, Germany) and relative density of the separated protein was quantified using ImageJ software.

2.4 | Immunofluorescence staining

Cells were fixed with 4% paraformaldehyde (Sigma), permeabilized with 0.5% Triton X-100 (Sigma) and incubated with 3% BSA (Sigma) and 10% FCS in PBS to block unspecific binding sites. After labeling antigens with primary antibodies, cells were incubated with the corresponding Alexa Fluor secondary antibodies (Thermo Fisher Scientific) and nuclear DNA was stained with 0.1 μg/ml DAPI (Sigma). Stained cells were viewed with an Olympus IX81/Fluoview FV1000 confocal laser-scanning microscope and imaged with the Olympus Fluoview 4.2 software. Diameters of ABCA3-HA containing vesicles in Z stack image series (height 0.4 μm) were determined with the ImageJ software tool. Volumes of 60 different ABCA3-HA vesicles chosen randomly from three distinct experiments were calculated with the formula $V = \frac{4}{3} * \pi * r^3$.

2.5 | Electron microscopy

Stable cells were fixed with 150 mM HEPES (pH 7.35) containing 1.5% formaldehyde and 1.5% glutaraldehyde (Sigma). After dehydration in acetone (Sigma), fixed cells were embedded in EPON and 50 nm sections were stained with 4% uranyl acetate and lead citrate. A Morgagni TEM (FEI) was used to study the sections. Images were taken with a 2 K side mounted Veleta CCD camera and analyzed by a scientist well experienced with the ultrastructure of LBs.

2.6 | Lipid analyses

Cells were lysed in SDS buffer (0.1% SDS, 1 mM EDTA in 0.1 M Tris pH7.4) for 15 min at room temperature. Protein concentrations of the lysates were measured and intracellular lipids were analyzed by ESI-MS/MS in positive ion mode as described previously (Griese et al., 2015b).

2.7 | Statistical analysis

Statistical analysis was performed using ordinary one-way ANOVA unless stated otherwise. Tukey's post hoc test for multiple comparisons was used to detect statistically significant differences between all group means. Only statistical differences between WT and the single variants are indicated in the graphs unless stated otherwise. *P* values < 0.05 were considered to be statistically significant. Results are presented as mean ± SEM of a minimum of three independent experiments. All tests were performed using Graph Pad Prism 6.0 (GraphPad Software, La Jolla, USA).

3 | RESULTS

3.1 | Generation of stable cell clones expressing ABCA3-HA WT and its variants

All ABCA3 sequence variations selected were previously observed in patients with varying severity of ILD (Supp. Table S1). Stably transfected A549 cell lines, overexpressing either ABCA3-HA WT or its selected variants at high ABCA3-HA mRNA levels compared with mock control cells, expressed ABCA3-HA protein at similar high levels (Supp. Figures S1 and S2). Solely p.M760R expressing cells showed lower mRNA and protein expression compared with ABCA3-HA WT and other variants. However, all measured differences in protein levels were not statistically significant. All cells transfected with ABCA3-HA showed an increase of cell metabolic activity over time similar to mock control cells (Supp. Figure S3). Cell cytotoxicity quantified by the amount of lactate dehydrogenase (LDH) released in cell supernatants did not differ between cells expressing ABCA3-HA WT, its variants and the mock control, except for p.M760R expressing cells with elevated levels of cell injury after a longer time span, that is, 96 hr (Supp. Figure S4).

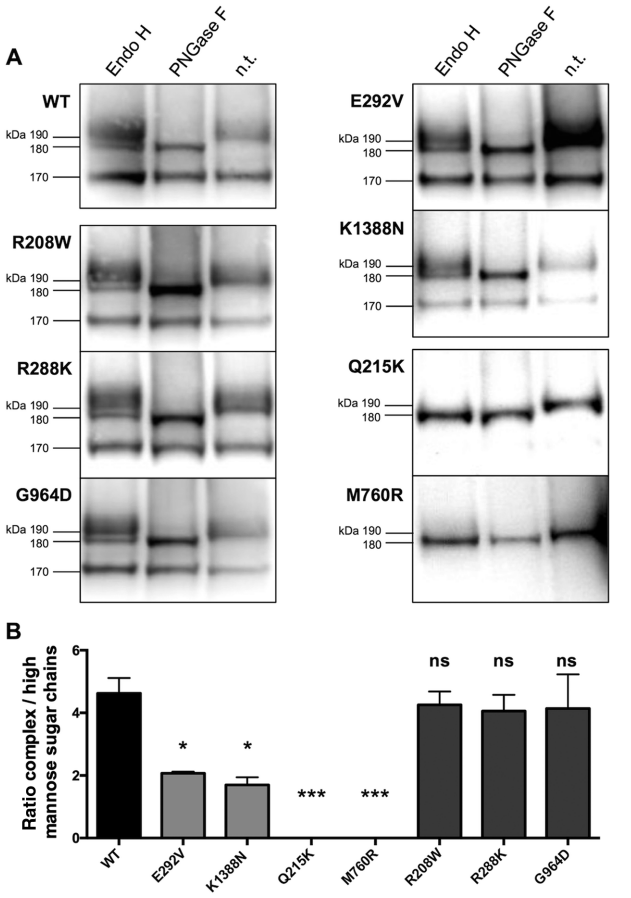

FIGURE 3 N-glycosylation of ABCA3-HA after digestion with EndoH or PNGaseF. **A**: The noncleaved 190 kDa protein is fully deglycosylated by PNGaseF, causing a shift in electrophoretic mobility to 180 kDa. EndoH digestion results in a separation of EndoH-sensitive 180 kDa protein (by cleaving high-mannose oligosaccharides) and EndoH-insensitive 190 kDa protein (with remaining complex-type oligosaccharides) in ABCA3 WT, p.R208W, p.R288K, p.G964D, p.E292V, and p.K1388N. The variants p.Q215K and p.M760R show only a single EndoH-sensitive 180 kDa ABCA3-HA protein band. Abbreviation "n.t." stands for nontreated control. Images of WT and p.K1388N have been published (Wittmann et al., 2016b). **B**: Ratio of complex-type oligosaccharides to high-mannose oligosaccharides (i.e., 190 to 180 kDa) in noncleaved ABCA3-HA protein quantified by relative densitometry using ImageJ. Ratios of p.Q215K and p.M760R were set to 0 since there was no insensitive band detectable ($n = 3$, $^{*}P < 0.05$, $^{***}P < 0.001$ compared with WT)

3.2 | Intracellular trafficking and localization of ABCA3-HA

The ABCA3-HA protein is N-glycosylated in the endoplasmic reticulum (ER) with high-mannose oligosaccharides, which are then modified to complex-type oligosaccharides in the Golgi apparatus. PNGaseF is an enzyme, which is able to cleave both types of oligosaccharides, whereas the enzyme EndoH only cleaves the high-mannose type oligosaccharides (Matsumura et al., 2006). Therefore the ABCA3-HA protein is fully deglycosylated following digestion with PNGaseF, which can be identified by a mobility shift from 190 to 180 kDa in immunoblotting. Digestion with EndoH however, is able to separate the sensitive 180 kDa protein (by cleaving high-mannose oligosaccharides) from the insensitive 190 kDa protein band with remaining complex-type oligosaccharides. N-glycosylation studies (Figure 3) revealed that ABCA3-HA proteins with the variants p.E292V, p.K1388N, p.R208W, p.R288K, and p.G964D were processed from high-mannose to complex-type oligosaccharides, indicating that all those proteins were correctly processed within the ER and Golgi apparatus. However, proteins with the variants p.E292V and p.K1388N showed a reduced ratio of complex to high-mannose oligosaccharides, which suggests that less protein was correctly processed compared with the WT. p.Q215K and p.M760R proteins contained no complex but only high-mannose oligosaccharides, indicating that these proteins did not reach the Golgi apparatus at all. As previously reported (Nagata et al., 2004), the lower 170 kDa protein band was not affected by digestion with neither PNGaseF nor EndoH, suggesting that this form of the ABCA3 protein is not glycosylated and possibly a product of degradation. Intracellular localization was directly investigated by immunofluorescence costaining of ABCA3-HA protein (green) with the lysosomal marker CD63 or the ER-resident chaperone Calnexin (both red) as shown in Figure 4. The protein variants p.E292V, p.K1388N, p.R208W, p.R288K, and p.G964D as well as the WT protein clearly colocalized with vesicular structures labeled by CD63, indicating that these proteins reached the limiting membrane of LBs. p.Q215K and p.M760R proteins showed a diffuse pattern throughout the whole cell without detectable vesicles or colocalization with CD63, illustrating that these protein variants might have failed to approach and form typical LBs. Unexpectedly, none of the p.Q215K and p.M760R protein colocalized with Calnexin.

3.3 | LB volume and morphology

The mean volume of vesicles stained by immunofluorescence, that is, LB like structures containing ABCA3-HA protein, was measured as described in the methods. Cells expressing p.R208W, p.R288K, and p.G964D ABCA3-HA showed the same mean vesicle volume as the ABCA3-HA WT, whereas vesicles in p.E292V and p.K1388N expressing cells were significantly smaller (Figure 5). Since A549 cells expressing the variants p.Q215K and p.M760R only showed a diffuse ABCA3-HA staining pattern but did not contain any detectable ABCA3-HA positive vesicular structures, the value for the corresponding volumes was set to 0 μm^3. LBs were directly visualized by electron microscopy (Figure 6). Although mock control cells contained no LBs at all, ABCA3-HA WT cells had well-organized LB like structures with parallel-arranged concentric membranes. Cells expressing the variants p.R208W, p.R288K, p.G964D similarly developed well-formed organelles comparable to ABCA3-HA WT cells, whereas organelles of p.E292V cells appeared to be smaller. p.K1388N, p.Q215K, and p.M760R expressing cells presented with abnormal, fried-egg-like structured LBs, which were also remarkably reduced within p.Q215K and p.M760R expressing cells.

3.4 | Intracellular phosphatidylcholine content

In order to gain an estimation of the ABCA3 transport function, intracellular total phosphatidylcholine (PC) content as well as

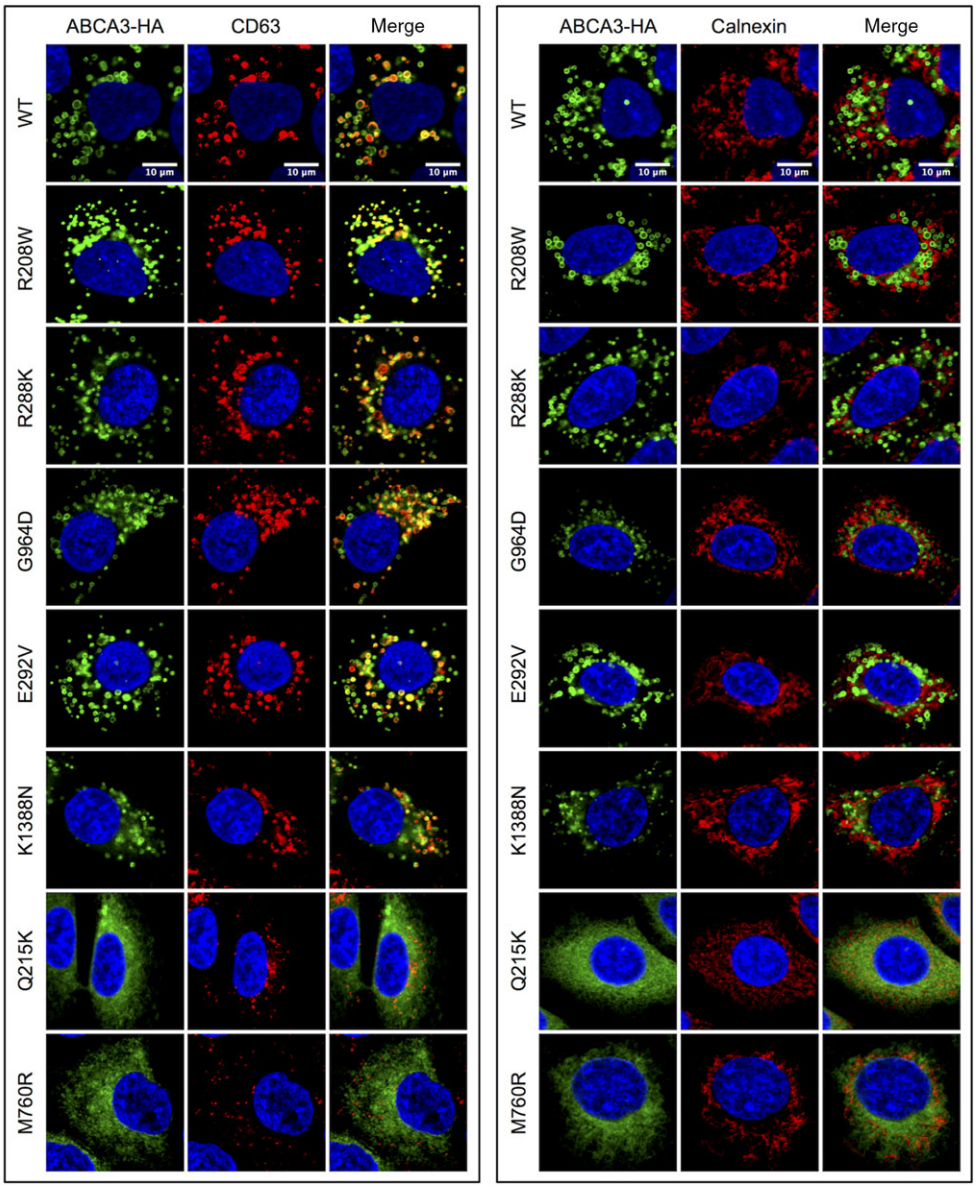

FIGURE 4 Immunofluorescence costaining of ABCA3-HA with CD63 or Calnexin. ABCA3-HA WT, p.R208W, p.R288K, p.G964D, p.E292V, and p.K1388N colocalize with CD63 but not Calnexin. ABCA3-HA p.Q215K and p.M760R show no colocalization with either CD63 or Calnexin. Scale bar equals 10 μm

dipalmitoylphosphatidylcholine (DPPC) as the main constituent of pulmonary surfactant were measured (Figure 7) (Ban et al., 2007; Nagata et al., 2004; Wittmann et al., 2016b). Cells expressing the variants p.R208W, p.R288K, and p.G864D showed similar levels of total PC and surfactant specific DPPC as WT cells. The expression of p.Q215K, p.M760R, p.E292V, and p.K1388N variants led to a significantly reduced intracellular total PC and an even greater decreased intracellular DPPC level, similar to mock control cells.

3.5 | Proteolytic cleavage of ABCA3-HA

It was recently shown that the ABCA3 protein undergoes N-terminal proteolytic cleavage by cathepsin L and B within the LBs, which most likely represents a form of ABCA3 degradation (Hofmann et al., 2016). This form of intracellular protein processing can be directly assessed through Immunoblotting since it results in a cleaved 170 kDa and a noncleaved 190 kDa protein band. ABCA3-HA WT protein and its variants p.R208W, p.R288K, p.G964D presented with similar intensity ratios of lower (170 kDa) to upper (190 kDa) protein band (Figure 8). Interestingly, the p.E292V protein had a ratio close to the WT ratio, whereas the p.K1388N protein only had a very small processed lower band and therefore a greatly reduced ratio. There was no processed lower band detectable for the p.Q215K and p.M760R protein and hence the intensity ratio obtained for these variants was 0.

4 | DISCUSSION

In this study, we defined the cellular phenotype of a collection of ABCA3 protein variants in comparison with the WT, while

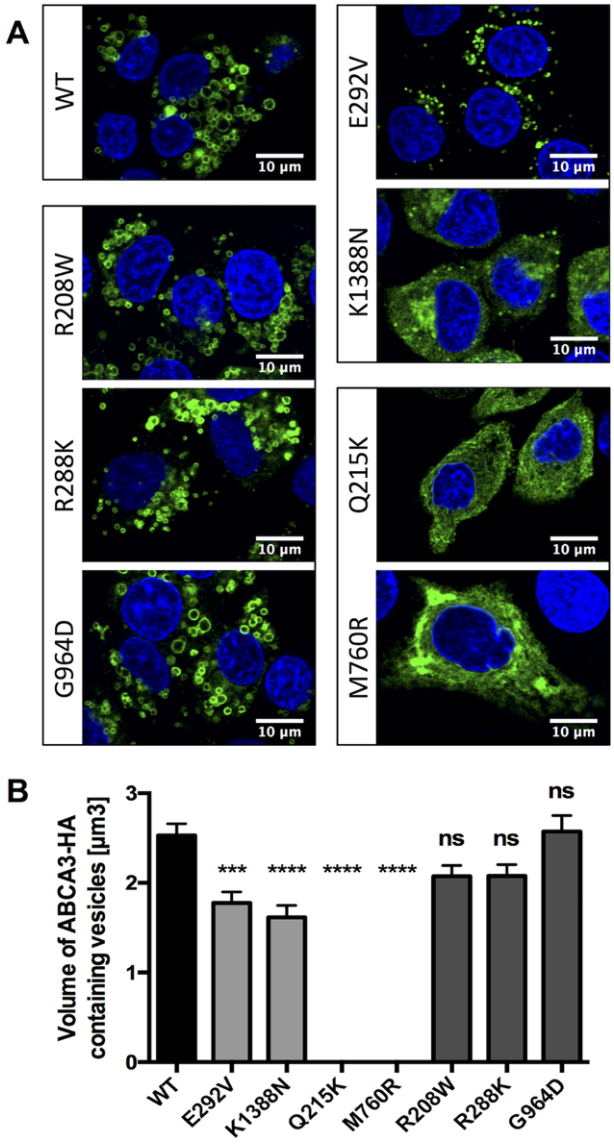

FIGURE 5 Volumes of LBs in A549 cells stably transfected with ABCA3-HA WT and variations. **A**: Immunofluorescence staining of ABCA3-HA protein in either vesicles (LBs of WT, p.R208W, p.R288K, p.G964D, p.E292V, and p.K1388N) or otherwise located inside the cell (p.Q215K and p.M760R). Scale bar equals 10 μm. **B**: Mean values of ABCA3-HA vesicle volumes. Values of p.Q215K and p.M760R were set to 0 μm^3 since there were no vesicles detectable ($n = 60$, $^{***}P < 0.001$, $^{****}P < 0.0001$ compared with WT)

focusing on nontruncating missense mutations with a single amino acid exchange only. We could differentiate variants with disrupted intracellular ABCA3 protein localization, variants impairing the lipid transport of ABCA3 protein and variants predisposing for the development of ILD by yet undetermined mechanisms despite correct localization and apparently normal lipid transport (Supp. Table S2).

4.1 | Variants with abnormal intracellular localization (i.e., trafficking defects)

In addition to the previously analyzed p.Q215K mutation (Engelbrecht, Kaltenborn, Griese, & Kern, 2010), we newly identified the ABCA3 sequence variation p.M760R to have a severe trafficking defect. The corresponding ABCA3 protein could not be detected within LB like structures and was completely lacking complex-type oligosaccharides, which typically mark the passage through the Golgi apparatus. These data are in agreement with the results of other ABCA3 trafficking mutations, for example, the variant c.302T > C, p.L101P (Matsumura et al., 2006). We could not prove the assumption that the mutant protein might have retained in the ER due to protein misfolding as previously described for trafficking defects (Cheong et al., 2006; Engelbrecht et al., 2010), since there was no apparent colocalization with Calnexin. In combination with the highly diffuse ABCA3-HA labeling pattern throughout the whole cell, this leads to the conclusion that the mutant ABCA3-HA protein might have somehow retained within the cytoplasm, similar as previously described for the ABCA4 (Sabirzhanova et al., 2015) and ABCC7 transporter (Du et al., 2015). An alternative explanation could be that this diffuse staining pattern is due to HA-containing ABCA3 remnants within the cytoplasm after protein degradation in the ER or any other form of transport out of the ER, for example. The few LBs that could be visualized by electron microscopy presented with an abnormal fried-egg-like structure, indicating malfunction. However, we detected sporadic well-developed LB like structures within the variant p.Q215K, suggesting that a very small amount of this protein possessed the potential to function correctly. Since the vast majority of p.Q215K and p.M760R protein did not localize correctly, hardly any phospholipid transport occurred to form LBs and no N-terminal proteolytic cleavage took place. Both mutations possibly undergo an alternative degradation pathway within the ER or the cytoplasm, if after all.

A full-term newborn with the homozygous combination of p.Q215K and p.R288K mutations presented with severe respiratory distress syndrome and early neonatal death, while its lung histology revealed a combined picture of idiopathic interstitial pneumonias as well as the existence of electron-dense bodies demonstrating ABCA3 malfunction (Brasch et al., 2006; Kroner et al., 2017). Since we could demonstrate the little cellular impact of the variant p.R288K, this severe phenotype is presumably due to an ABCA3 trafficking defect mediated by the p.Q215K variation. Another full-term newborn, reported to be compound heterozygous for the mutations p.M760R and p.R208W, similarly presented with early respiratory failure, electron-dense bodies and progressive interstitial pneumonitis until receiving a lung transplant at the age of 5 years (Doan et al., 2008). Even though we would only expect a sparse impact of the variant p.R208W, its remaining protein function apparently could not fully compensate for the heavy trafficking defect encoded by the variant p.M760R on the other allele. These cases prove the close correlation of our in vitro and existing ex vivo data.

4.2 | Variants with correct intracellular localization, but impaired lipid transport

The previously described variant p.E292V and our known control p.K1388N were correctly processed within the ER and Golgi apparatus as complex-type oligosaccharides within the protein were detected. Surprisingly, the ratio of complex to high-mannose

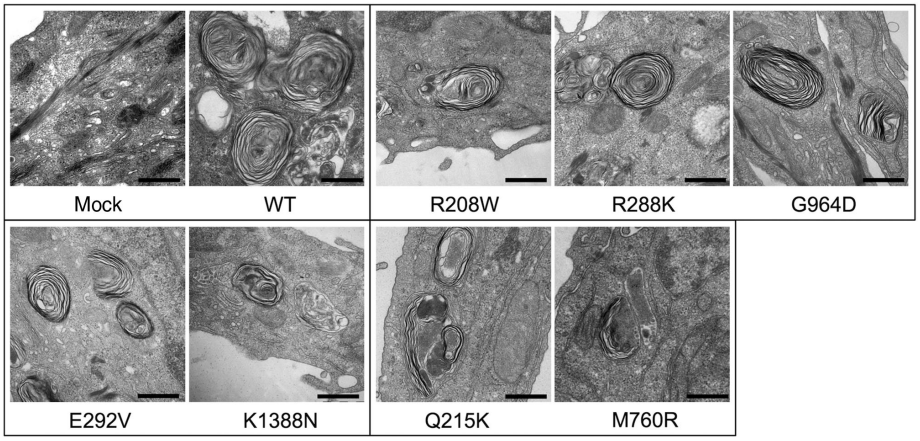

FIGURE 6 Transmission electron microscopy of LBs induced in A549 cells by stable transfection with mock control, ABCA3-HA WT, p.R208W, p.Q215K, p.R288K, p.E292V, p.M760R, p.G964D, and p.K1388N. Scale bar equals 0.5 μm. Images of mock control, WT, and p.K1388N have been published (Wittmann et al., 2016b)

oligosaccharides was reduced in comparison with the WT protein, suggesting that less of the variant protein has actually passed the Golgi apparatus. Immunofluorescence staining revealed the correct localization of p.E292V and p.K1388N protein in LB like structures, which however appeared to be much smaller compared with the WT. Electron microscopy of cells expressing the p.K1388N variant additionally showed abnormal fried-egg-like structured LBs, very likely indicating dysfunction. Höppner et al. (2017) recently developed a new method, which consistently identified a reduced lipid amount within LBs of the p.K1388N but not the p.E292V variant. Nevertheless, p.E292V cells presented with a lower percentage of filled vesicles in total, indicating that LB formation and overall transport activity was also harmed (Höppner et al., 2017). The variant p.E292V, which is located within a cytosolic loop adjacent to the NBD1 domain, has previously been described as type 2 mutation with an only moderately preserved lipid transport activity (Matsumura et al., 2006; Matsumura, Ban, & Inagaki, 2008). The significantly reduced intracellular amounts of total PC and DPPC in p.K1388N as well as p.E292V further support the theory that both variants suffer from an impaired lipid transport. Since the crucial role of ABCA3 protein is phospholipid transport into LBs, we decided to perform intracellular lipid analysis as a functional assay for classification (Wittmann et al., 2016b), while an additional analysis of ATP hydrolysis could provide further evidence for transport defects. Interestingly, we noticed a very weak diffuse ABCA3-HA staining pattern in the background of the p.K1388N variant cell, which did not colocalize with the ER. Thus we concluded that, if a small part of this mutant protein is not correctly processed, it might also accumulate in the cytoplasm as discussed above. Proteolytic cleavage of ABCA3-HA did occur in both variants, albeit at a lower level within p.K1388N, which could be in consistence with the small amount of presumably mislocalized p.K1388N protein.

Two infants with homozygous p.E292V mutations both presented with severe respiratory distress syndrome. One died shortly after birth (Wambach et al., 2014), the other one was still alive at the age of 2 years despite poor response to the clinical treatment (Turcu, Ashton, Jenkins, Gupta, & Mok, 2013). Interestingly, an adult with idiopathic pulmonary fibrosis was also identified to be homozygous for the p.E292V

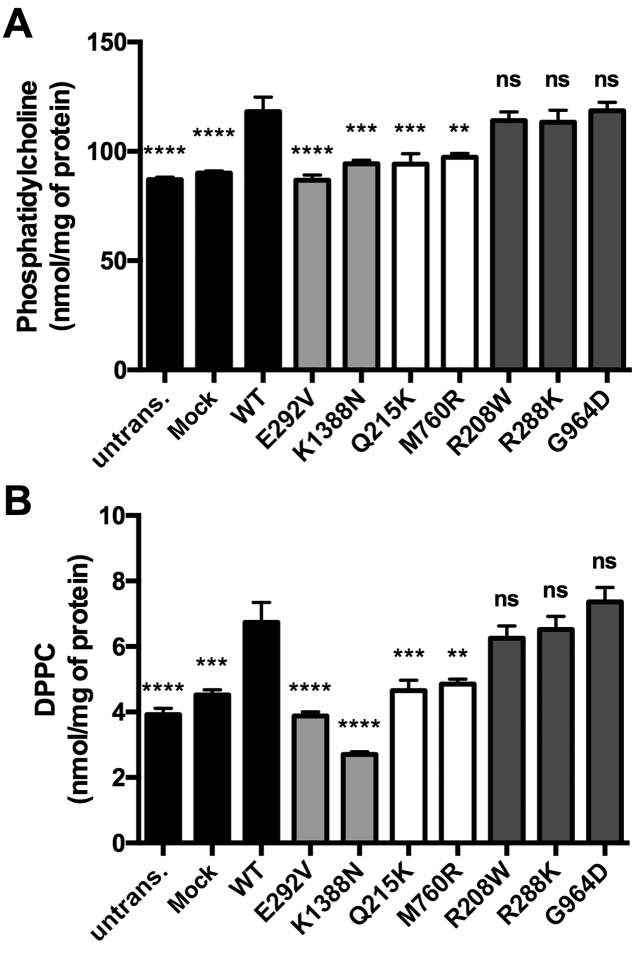

FIGURE 7 Intracellular PC analysis of untransfected A549 and mock control cells, ABCA3-HA WT, and variants. **A**: Intracellular total PC content of untransfected A549 and mock control cells, as well as A549 cells stably transfected with ABCA3-HA WT, p.R208W, p.Q215K, p.R288K, p.E292V, p.M760R, p.G964D, and p.K1388N ($n = 9$, $^{*}P < 0.05$, $^{**}P < 0.01$, $^{****}P < 0.0001$ compared with WT). **B**: Intracellular DPPC content of untransfected A549 and mock control cells, as well as stably transfected A549 cells ($n = 9$, $^{**}P < 0.01$, $^{****}P < 0.0001$ compared with WT). Data of WT and p.K1388N have been published (Wittmann et al., 2016b)

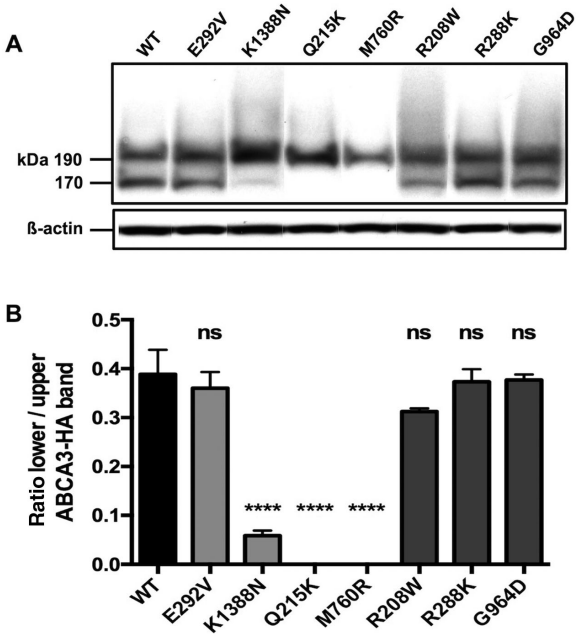

FIGURE 8 Proteolytic cleavage of ABCA3-HA protein. **A**: Immunoblot analysis of ABCA3-HA protein in total cell lysates with loading control β-actin. **B**: Intensity ratio of cleaved lower (170 kDa) to noncleaved upper (190 kDa) protein band. Ratios of p.Q215K and p.M760R were set to 0 since there was no lower band detectable ($n = 6$, $^{****}P < 0.0001$ compared with WT)

mutation (Coghlan et al., 2014), demonstrating the broad range of clinical outcomes possible. Thus more clinical data need to be collected to describe the phenotype of this variant. A young patient, expressing the novel p.K1388N mutation in a homozygous manner, also suffered from neonatal severe respiratory distress syndrome followed by chronic pneumonitis of infancy and early post-neonatal death (Wittmann et al., 2016b). The lethal outcome in these cases emphasizes the dysfunction of ABCA3 protein despite its correct intracellular localization and again supports the validity of our obtained in vitro results.

4.3 | Variants with yet undefined pathomechanisms predisposing for the development of ILD

The previously described p.R288K and p.G964D variants, as well as the newly investigated variant p.R208W show correct protein processing and intracellular localization, well-formed LB like structures due to sufficient lipid transport and regular proteolytic cleavage comparable to the WT. Nevertheless, patients carrying these mutations in a homo- or heterozygous manner presented with neonatal mild respiratory distress syndrome or ILD in later life. For example, Campo et al. (2014) described the case of a girl, homozygously expressing the p.G964D variant, who was diagnosed with usual interstitial pneumonia fairly late in her youth. A group of children carrying the p.R288K variant in a heterozygous manner all presented with neonatal respiratory insufficiency and developed chronic ILD during their early childhood (Wittmann et al., 2016a). As reported above, a newborn heterozygous for the mutations p.M760R and p.R208W also experienced early respiratory failure, indicating that the variant p.R208W was not capable to compensate for the heavy trafficking defect encoded by the p.M760R variant on the other allele (Doan et al., 2008).

Based on these clinical observations, we think that the variants p.R208W, p.R288K, and p.G964D predispose for the development of ILD by yet undefined mechanisms that cannot be classified into neither type 1 nor type 2 mutations. The underlying pathologies of these variations appear to be less severe, but the possible combination with previous initial lung injury (Kaltenborn et al., 2012; Wittmann et al., 2016a) or a longer time span during which interstitial injury and fibrosis might arise (Campo et al., 2014) may result in chronic ILD. Such differences are also more difficult to detect. For example, a direct comparison between the WT and p.R288K variant in vitro shows very small differences, i.e. 20% smaller LBs (Wittmann et al., 2016a), which are not detectable within the multiple comparisons performed in the current analysis. Regarding the variant p.G964D, we also did not detect differences in intracellular lipid contents as it has been previously described (Campo et al., 2014). This discrepancy, as well as the more variable appearing organization of LB like structures reported in electron microscopy, is most likely due to the only small effects on overall cellular lipid composition and the use of the different cell line HEK293 in the previous study.

A recent study by Wambach et al. (2016) confirmed our observations regarding intracellular trafficking and processing of the ABCA3 variant p.R288K. In their study, the protein variant p.R288K showed a somewhat reduced ATPase activity compared with WT and a normal biogenesis of LB like structures (Wambach et al., 2016). These findings suggest that a reduced ATP hydrolysis does not necessarily disrupt the formation of LB like structures and therefore overall ABCA3 lipid transport. Consistently, we measured comparable intracellular PC levels in cells stably transfected with the ABCA3 WT and p.R288K variants. This reported underlying pathomechanism seems to have only little cellular impact, but might be accountable for the clinical outcome of affected patients in the long run or during acute respiratory distress. Additional other pathomechanisms within some of these mutations could be linked to an increased rate of apoptosis due to some ER stress, caused by ABCA3 variants which are partially ER localized, as previously reported (Weichert et al., 2011). In individual subjects many other genetic and environmental factors and associated disease mechanisms may modify the expression of all identified ABCA3 variants.

4.4 | Limitations and weaknesses of the study

We used the human A549 cell line to generate stable ABCA3 expressing cell models for our in vitro studies. Certainly, the most reliable cell model would have been patient-derived type II pneumocytes homozygously carrying the chosen sequence variations. An alternative model might be human induced pluripotent stem cells with and without these point mutations. Unfortunately, such cells are currently not available, but could be used in future to reproduce and therapeutically target these genetic defects.

When selecting our stably transfected ABCA3-HA A549 cell clones, we took care that they expressed comparable levels of ABCA3-HA mRNA and protein. Of note is variant p.M760R, which had about 50% lower mRNA levels even in best performing clones and likely

reduced p.M760R protein levels, albeit no significant differences were detected here (Supp. Figures S1 and S2). This variant results in a severe trafficking defect, potentially inducing ER stress and leaving the cells more vulnerable, as demonstrated in our analysis of cell cytotoxicity. The specific mechanisms by which trafficking mutations lead to cellular damage need to be further investigated.

It was impossible to isolate LBs for lipid analysis by standard methods because these organelles may not or only incompletely be formed depending on the cells' mutation. However, since DPPC represents the major surfactant PC species in type II pneumocytes (Nagata et al., 2004), our lipid analysis of whole cell extracts gives important clues to the extent of normal surfactant synthesis (Griese et al., 2015b; Wittmann et al., 2016a; Wittmann et al., 2016b). Due to the overexpression of ABCA3 protein in our stably transfected cells, we assume that the enhanced transport of PC and especially DPPC into LBs does have a noticeable impact on the overall lipid homeostasis and therefore also affects total intracellular lipid contents. As DPPC is mainly secreted into the extracellular alveolar space within LBs (Griese, 1999), we tried to determine this particular species in the supernatant of our cultured cells. However, the sensitivity of mass spectrometry was too low to reliably detect it (data not shown). Besides, we found no up-to-date evidence that A549 cells, initially isolated over 40 years ago, still possess the ability to actually release their LB content.

5 | SUMMARY

We have analyzed the cellular consequences of selected ABCA3 sequence variations and developed an enhanced classification system using a particular set of criteria. The allocation of distinct ABCA3 variants into groups with the same molecular defects is an important step toward a further understanding of the underlying pathomechanisms. Already available small molecule correctors could specifically target ABCA3 variations in such defined groups, whereas secondary prevention by avoiding additional external lung stressors might be the major aim for other groups. We think a convenient classification system of ABCA3 variants helps to forecast the clinical outcome of affected patients and eventually to develop specific repair mechanisms for future in vitro and in vivo application.

DECLARATIONS

Ethics approval and consent to participate: The usage of patient data and materials was prospectively reviewed and approved by the Ethical Review Committee of the Ludwig-Maximilians University Munich, Germany (EK 111–13).

Consent for publication: All caregivers of the participants gave their informed consent to use their data and materials for this work.

AUTHORS' CONTRIBUTIONS

U.S., T.W., and M.G. designed the study, analyzed data, and wrote the manuscript. U.S., T.W., S.H., S.K., G.L., and J.H. performed the research, contributed important reagents, and analyzed data. M.G. is responsible for the study content and validity of the data. All authors have read and approved the final manuscript. This work contains parts of the medical thesis of U.S.

ACKNOWLEDGMENTS

We thank Kathrin Schiffl and Andrea Schams for their excellent technical assistance and Dr. Ralf Zarbock for many helpful discussions.

DISCLOSURE STATEMENT

The authors declare no conflict of interest.

ORCID

Matthias Griese http://orcid.org/0000-0003-0113-912X

REFERENCES

Ban, N., Matsumura, Y., Sakai, H., Takanezawa, Y., Sasaki, M., Arai, H., & Inagaki, N. (2007). ABCA3 as a lipid transporter in pulmonary surfactant biogenesis. *Journal of Biological Chemistry*, *282*(13), 9628–9634. doi:10.1074/jbc.M611767200

Beers, M. F., & Mulugeta, S. (2017). The biology of the ABCA3 lipid transporter in lung health and disease. *Cell Tissue Research*, *367*(3), 481–493. doi:10.1007/s00441-016-2554-z

Besnard, V., Matsuzaki, Y., Clark, J., Xu, Y., Wert, S. E., Ikegami, M., … Whitsett, J. A. (2010). Conditional deletion of Abca3 in alveolar type II cells alters surfactant homeostasis in newborn and adult mice. *American Journal of Physiology-Lung Cellular andMolecular Physiology*, *298*(5), L646–659. doi:10.1152/ajplung.00409.2009

Brasch, F., Schimanski, S., Muhlfeld, C., Barlage, S., Langmann, T., Aslanidis, C., … Schmitz, G. (2006). Alteration of the pulmonary surfactant system in full-term infants with hereditary ABCA3 deficiency. *American Journal of Respiratory and Critical Care Medicine*, *174*(5), 571–580. doi:10.1164/rccm.200509-1535OC

Campo, I., Zorzetto, M., Mariani, F., Kadija, Z., Morbini, P., Dore, R., … Luisetti, M. (2014). A large kindred of pulmonary fibrosis associated with a novel ABCA3 gene variant. *Respiratory Research*, *15*, 43. doi:10.1186/1465-9921-15-43

Cheong, N., Madesh, M., Gonzales, L. W., Zhao, M., Yu, K., Ballard, P. L., & Shuman, H. (2006). Functional and trafficking defects in ATP binding cassette A3 mutants associated with respiratory distress syndrome. *Journal of Biological Chemistry*, *281*(14), 9791–9800. doi:10.1074/jbc.M507515200

Cheong, N., Zhang, H., Madesh, M., Zhao, M., Yu, K., Dodia, C., … Shuman, H. (2007). ABCA3 is critical for lamellar body biogenesis in vivo. *Journal of Biological Chemistry*, *282*(33), 23811–23817. doi:10.1074/jbc.M703927200

Coghlan, M. A., Shifren, A., Huang, H. J., Russell, T. D., Mitra, R. D., Zhang, Q., … Hamvas, A. (2014). Sequencing of idiopathic pulmonary fibrosis-related genes reveals independent single gene associations. *BMJ Open Respiratory Research*, *1*(1), e000057. doi:10.1136/bmjresp-2014-000057

Doan, M. L., Guillerman, R. P., Dishop, M. K., Nogee, L. M., Langston, C., Mallory, G. B., … Fan, L. L. (2008). Clinical, radiological and pathological features of ABCA3 mutations in children. *Thorax*, *63*(4), 366–373. doi:10.1136/thx.2007.083766

Du, K., Karp, P. H., Ackerley, C., Zabner, J., Keshavjee, S., Cutz, E., & Yeger, H. (2015). Aggregates of mutant CFTR fragments in airway epithelial cells of CF lungs: New pathologic observations. *Journal of Cystic Fibrosis*, *14*(2), 182–193. doi:10.1016/j.jcf.2014.09.012

Engelbrecht, S., Kaltenborn, E., Griese, M., & Kern, S. (2010). The surfactant lipid transporter ABCA3 is N-terminally cleaved inside

LAMP3-positive vesicles. *FEBS Letters*, *584*(20), 4306–4312. doi:10.1016/j.febslet.2010.09.026

Flamein, F., Riffault, L., Muselet-Charlier, C., Pernelle, J., Feldmann, D., Jonard, L., … Guillot, L. (2012). Molecular and cellular characteristics of ABCA3 mutations associated with diffuse parenchymal lung diseases in children. *Human Molecular Genetics*, *21*(4), 765–775. doi:10.1093/hmg/ddr508

Geurts, A. M., Yang, Y., Clark, K. J., Liu, G., Cui, Z., Dupuy, A. J., … Hackett, P. B. (2003). Gene transfer into genomes of human cells by the sleeping beauty transposon system. *Molecular Therapy*, *8*(1), 108–117.

Griese, M. (1999). Pulmonary surfactant in health and human lung diseases: State of the art. *European Respiratory Journal*, *13*(6), 1455–1476.

Griese, M., Irnstetter, A., Hengst, M., Burmester, H., Nagel, F., Ripper, J., … Kroner, C. (2015a). Categorizing diffuse parenchymal lung disease in children. *Orphanet Journal of Rare Diseases*, *10*(1), 122. doi:10.1186/s13023-015-0339-1

Griese, M., Kirmeier, H. G., Liebisch, G., Rauch, D., Stuckler, F., & Schmitz, G. (2015b). … KILD-BAL Working Group of the Kids-Lung-Register. Surfactant lipidomics in healthy children and childhood interstitial lung disease. *PLoS One*, *10*(2), e0117985. doi:10.1371/journal.pone.0117985

Griese, M., Lorenz, E., Hengst, M., Schams, A., Wesselak, T., Rauch, D., … Zarbock, R. (2016). Surfactant proteins in pediatric interstitial lung disease. *Pediatric Research*, *79*(1-1), 34–41. doi:10.1038/pr.2015.173

Hartl, D., & Griese, M. (2005). Interstitial lung disease in children—Genetic background and associated phenotypes. *Respiratory Research*, *6*, 32. doi:10.1186/1465-9921-6-32

Hofmann, N., Galetskiy, D., Rauch, D., Wittmann, T., Marquardt, A., Griese, M., & Zarbock, R. (2016). Analysis of the proteolytic processing of ABCA3: Identification of cleavage site and involved proteases. *PLoS One*, *11*(3), e0152594. doi:10.1371/journal.pone.0152594

Höppner, S., Kinting, S., Torrano, A. A., Schindlbeck, U., Brauchle, C., Zarbock, R., … Griese, M. (2017). Quantification of volume and lipid filling of intracellular vesicles carrying the ABCA3 transporter. *Biochimica et Biophysica Acta*, *1864*(12), 2330–2335. doi:10.1016/j.bbamcr.2017.08.013

Kaltenborn, E., Kern, S., Frixel, S., Fragnet, L., Conzelmann, K. K., Zarbock, R., & Griese, M. (2012). Respiratory syncytial virus potentiates ABCA3 mutation-induced loss of lung epithelial cell differentiation. *Human Molecular Genetics*, *21*(12), 2793–2806. doi:10.1093/hmg/dds107

Kleinlein, B., Griese, M., Liebisch, G., Krude, H., Lohse, P., Aslanidis, C., … Holzinger, A. (2011). Fatal neonatal respiratory failure in an infant with congenital hypothyroidism due to haploinsufficiency of the NKX2-1 gene: Alteration of pulmonary surfactant homeostasis. *Archives of Disease in Childhood. Fetal and Neonatal Edition*, *96*(6), F453–456. doi:10.1136/adc.2009.180448

Kroner, C., Wittmann, T., Reu, S., Teusch, V., Klemme, M., Rauch, D., … Griese, M. (2017). Lung disease caused by ABCA3 mutations. *Thorax*, *72*(3), 213–220. doi:10.1136/thoraxjnl-2016-208649

Matsumura, Y., Ban, N., & Inagaki, N. (2008). Aberrant catalytic cycle and impaired lipid transport into intracellular vesicles in ABCA3 mutants associated with nonfatal pediatric interstitial lung disease. *American Journal of Physiology-Lung Cellular and Molecular Physiology*, *295*(4), L698–707. doi:10.1152/ajplung.90352.2008

Matsumura, Y., Ban, N., Ueda, K., & Inagaki, N. (2006). Characterization and classification of ATP-binding cassette transporter ABCA3 mutants in fatal surfactant deficiency. *Journal of Biological Chemistry*, *281*(45), 34503–34514. doi:10.1074/jbc.M600071200

Nagata, K., Yamamoto, A., Ban, N., Tanaka, A. R., Matsuo, M., Kioka, N., … Ueda, K. (2004). Human ABCA3, a product of a responsible gene for abca3 for fatal surfactant deficiency in newborns, exhibits unique ATP hydrolysis activity and generates intracellular multilamellar vesicles. *Biochemical and Biophysical Research Communication*, *324*(1), 262–268. doi: 10.1016/j.bbrc.2004.09.043

Nogee, L. M. (2004). Alterations in SP-B and SP-C expression in neonatal lung disease. *Annual Review of Physiology*, *66*, 601–623. doi:10.1146/annurev.physiol.66.032102.134711

Sabirzhanova, I., Lopes Pacheco, M., Rapino, D., Grover, R., Handa, J. T., Guggino, W. B., & Cebotaru, L. (2015). Rescuing trafficking mutants of the ATP-binding cassette protein, ABCA4, with small molecule correctors as a treatment for Stargardt eye disease. *Journal of Biological Chemistry*, *290*(32), 19743–19755. doi:10.1074/jbc.M115.647685

Saugstad, O. D., Hansen, T. W. R., Rønnestad, A., Nakstad, B., Tølløfsrud, P. A., Reinholt, F., … Nogee, L. M. (2007). Novel mutations in the gene encoding ATP binding cassette protein member A3 (ABCA3) resulting in fatal neonatal lung disease. *Acta Paediatrica*, *96*(2), 185–190. doi:10.1111/j.1651-2227.2007.00016.x

Shulenin, S., Nogee, L. M., Annilo, T., Wert, S. E., Whitsett, J. A., & Dean, M. (2004). ABCA3 gene mutations in newborns with fatal surfactant deficiency. *New England Journal of Medicine*, *350*(13), 1296–1303. doi:10.1056/NEJMoa032178

Thorwarth, A., Schnittert-Hubener, S., Schrumpf, P., Muller, I., Jyrch, S., Dame, C., … Krude, H. (2014). Comprehensive genotyping and clinical characterisation reveal 27 novel NKX2-1 mutations and expand the phenotypic spectrum. *Journal of Medical Genetics*, *51*(6), 375–387. doi:10.1136/jmedgenet-2013-102248

Turcu, S., Ashton, E., Jenkins, L., Gupta, A., & Mok, Q. (2013). Genetic testing in children with surfactant dysfunction. *Archives of Disease in Childhood*, *98*(7), 490–495. doi:10.1136/archdischild-2012-303166

Wambach, J. A., Casey, A. M., Fishman, M. P., Wegner, D. J., Wert, S. E., Cole, F. S., … Nogee, L. M. (2014). Genotype-phenotype correlations for infants and children with ABCA3 deficiency. *American Journal of Respiratory and Critical Care Medicine*, *189*(12), 1538–1543. doi:10.1164/rccm.201402-0342OC

Wambach, J. A., Yang, P., Wegner, D. J., Heins, H. B., Kaliberova, L. N., Kaliberov, S. A., … Cole, F. S. (2016). Functional characterization of ATP-binding cassette transporter A3 mutations from infants with respiratory distress syndrome. *American Journal of Respiratory Cell and Molecular Biology*, *55*(5), 716–721. doi:10.1165/rcmb.2016-0008OC

Weichert, N., Kaltenborn, E., Hector, A., Woischnik, M., Schams, A., Holzinger, A., … Griese, M. (2011). Some ABCA3 mutations elevate ER stress and initiate apoptosis of lung epithelial cells. *Respiratory Research*, *12*, 4. doi:10.1186/1465-9921-12-4

Wittmann, T., Frixel, S., Höppner, S., Schindlbeck, U., Schams, A., Kappler, M. V., … Griese, M. (2016a). Increased risk of interstitial lung disease in children with a single R288K variant of ABCA3. *Molecular Medicine*, doi:10.2119/molmed.2015.00244

Wittmann, T., Schindlbeck, U., Höppner, S., Kinting, S., Frixel, S., Kroner, C., … Griese, M. (2016b). Tools to explore ABCA3 mutations causing interstitial lung disease. *Pediatric Pulmonology*, *51*(12), 1284–1294. doi:10.1002/ppul.23471

Yamano, G., Funahashi, H., Kawanami, O., Zhao, L. X., Ban, N., Uchida, Y., … Inagaki, N. (2001). ABCA3 is a lamellar body membrane protein in human lung alveolar type II cells. *FEBS Letters*, *508*(2), 221–225.

SUPPORTING INFORMATION

Additional Supporting Information may be found online in the supporting information tab for this article.

How to cite this article: Schindlbeck U, Wittmann T, Höppner S, et al. ABCA3 missense mutations causing surfactant dysfunction disorders have distinct cellular phenotypes. *Human Mutation*. 2018;39:841–850. https://doi.org/10.1002/humu.23416